An Open-Source Robotic Tool for the Simulation of Quasi-Static Finger Pressing on Stationary and Vibrating Surfaces

Yuri De Pra, Stefano Papetti, *Member, IEEE*, Federico Fontana, *Senior Member, IEEE*, and Emidio Tiberi

***Abstract*—The *Bogus Finger* is a remote-controllable tool for simulating vertical pressing forces of various magnitude as exerted by a human finger. Its main application is the characterization of haptic devices under realistic active touch conditions. The device is released as an open-source hardware and software DIY project that can be easily built using off-the-shelf components. We report the characterization of the quasi-static properties of the device, and validate its dynamic response to pressing on a vibrating surface by comparison with human fingers. The present prototype configuration accurately reproduces the mechanical impedance of the human finger in the frequency range 200–400 Hz.**

***Index Terms*—Haptic interfaces, vibration measurement, damping, finger pressing, interactive systems**

I. Introduction

FINGER pressing is a key gesture in our interaction with everyday devices. More in general, active touch has recently become a hot topic in haptics research, with important application outcomes reaching the consumer level (e.g., more and more sophisticated haptic sensing and actuation in mobile devices), in parallel stimulating studies on the psychophysics, physiology and mechanics of touch in interactive contexts [1], [2].

When conducting experiments on active touch or designing and characterizing haptic devices, several factors would motivate the use of an automated tool modeling the effect of a pressing finger while offering accurate vibration measurements. Tests with human participants involving active touch inherently prevent full control over the subjects' posture and gesture, thus posing various challenges in terms of measurement repeatability and accuracy [3]. This is generally reflected in highly variable and noisy results, not ascribable solely to the constitutional variability of human physiology [1], [4], [5]. Also, certain tests may require the implementation of special environmental conditions (e.g., vacuum chambers for friction assessment) incompatible with human participants. In the those scenarios, a robotic tool as described above would allow to ascertain the vibratory stimuli reaching the finger's mechanoreceptors under conditions equivalent to those of actual finger pressing, yet without employing human participants.

Then again, a rigorous characterization of the vibratory response of haptic devices targeting finger-based interaction (including experimental apparatuses) requires to take into account the effects induced by contacting fingers. Although the mass of a small accelerometer attached to the device in question can already emulate the inertia of a finger [6], [7], its stiffness and damping effects cannot be easily reproduced, especially if non-negligible pressing forces are involved. In fact, the compression of the fingertip pulp affects the related stiffness, damping and contact area, hence changing the impedance at the contact point [8]. A robotic tool that accurately simulates the mechanical characteristics of a pressing finger, paired with an accelerometer, would make it possible to obtain repeatable and stable reference measurements of the average vibratory or static response to finger interaction.

In order to address the use cases pointed out above, we developed the *Bogus Finger*: a robotic tool for the simulation of quasi-static finger-pressing forces of various magnitude, suitable for interaction with both stationary and vibrating surfaces. Since our main focus is the investigation of vibrotactile feedback in the range of highest human sensitivity [9], at this stage our prototype targets the reproduction of the mechanical impedance of the finger in the 200–400 Hz range. The device was recently employed for characterizing a vibrotactile surface for musical expression [10].

The fingertip pulp is usually modeled as a viscoelastic nonlinear spring-mass-damper mechanical system [6], whose impedance changes with the frequency and motion direction of external stimuli [11]. As motion direction is concerned, fingertips are anisotropic, exposing a different mechanical impedance in tangential and normal directions [12]. With regard to frequency, fingertips behave elastically up to about 100 Hz, while damping dominates up to 1 kHz; inertial contributions, instead, are negligible up to 500 Hz [7]. Those mechanical properties have been modeled through multiple

Manuscript received January 6, 2021; revised March 21, 2021; accepted April 24, 2021. Date of publication April 27, 2021; date of current version June 16, 2021. This research is part of project HAPTEEV (Haptic technology and evaluation for digital musical interfaces) funded by the Swiss National Science Foundation (under Grant 178972). The work of Yuri De Pra was supported by a scholarship of The Research Hub by Electrolux Professional SpA. *(Corresponding author: Yuri De Pra.)*

Yuri De Pra and Federico Fontana are with the Department of Mathematics, Computer Science and Physics, University of Udine, 3310 Udine, Italy (e-mail: yuri.depra@uniud.it; federico.fontana@uniud.it).

Stefano Papetti is with the Institute for Computer Music and Sound Technology, Zurich University of the Arts, 8005 Zurich, Switzerland (e-mail: stefano.papetti@zhdk.ch).

Emidio Tiberi is with the The Research Hub of Electrolux Professional SpA, Italy (e-mail: emidio.tiberi@electroluxprofessional.com).

Digital Object Identifier 10.1109/TOH.2021.3076052

measurements with humans, highlighting large variance among subjects even under controlled conditions [5], [7], [11].

Several models of finger contact have been proposed [13]–[16], as well as physical finger-analogue implementations [17], [18] mainly aimed at enabling robotic tactile sensing [19]. Among others, Fenton Friesen *et al.* [20] compared different types of complex artificial fingers consisting of bone, tissue, skin and outer skin layers analogues, while Controzzi *et al.* [21] built a bio-inspired artificial finger described by finite element modeling.

Insofar as existing artificial fingers offer accurate reproductions, they target quasi-static interface properties (e.g., surface friction and stiffness) rather than the response to dynamic stimuli such as those due to contact with vibrating objects. By contrast, the *Bogus Finger* can also reproduce finger pressing under dynamic conditions by simulating the impedance of the human finger when exposed to either normal or tangential vibration. Also, our tool was conceived as an inexpensive DIY device and is made available as an open-source project, making it a viable solution for a larger research community.

In what follows, a technical description of the *Bogus Finger* is first provided, including design and implementation solutions, followed by its characterization under static conditions and a validation that compared its dynamic response to that of real pressing fingers.

II. Device

Fig. 1(a) shows a working prototype of the *Bogus Finger* realized by assembling off-the-shelf components and custom-designed parts. The device is released as an open-source project (CC BY-NC 4.0) documented by a public repository linked to GitHub.[1] The repository stores DIY instructions, mechanical and electronic specifications and schematics, 3D models, Arduino code and Python script examples for remote control.

A. Hardware Design

The vertical displacement of the *Bogus Finger*'s end-effector is operated by a slide stroke linear motion actuator: a $250 \times 50 \times 50\,\mathrm{mm}$ vertical metal profile holds the actuator, whose motor (NEMA17 42 mm stepper motor, torque 4.5 kg $\cdot$ cm) is controlled by a TB6600 driver connected to an Arduino Mega 2560 microcontroller board. The driver also limits the current provided to the motor, in this way protecting it, and can increase its spatial accuracy by subdividing the motor's step into up to 32 sub-steps (maximum resolution 0.6 μm). A force signal read by a load-cell mounted on the end-effector is fed back into the microcontroller, allowing to reach and hold stable target forces over time.

The end-effector was designed to model a human finger pressing down vertically. Its components were selected among off-the-shelf material, aiming to match the mechanical properties of the finger as described in the literature [22]. Fig. 1(b) shows a schematic of the end-effector, whose main components are:

[1] https://github.com/yuridepra88/Bogus-Finger

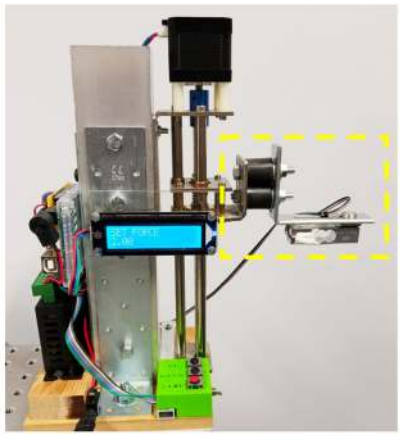

(a) Full view with end-effector surrounded by a yellow dashed line.

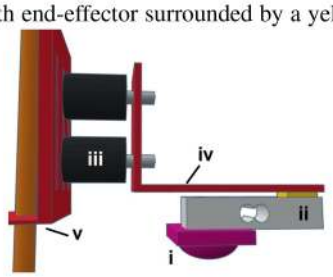

(b) End-effector schematic: hemispheric silicone layer (i), load-cell force sensor (ii), rubber shock-absorbers (iii), angle metal bracket (iv), vertically sliding metal plate (v).

Fig. 1. The *Bogus Finger*. (a) Full view with end-effector surrounded by a yellow dashed line. (b) End-effector schematic: hemispheric silicone layer (i), load-cell force sensor (ii), rubber shock-absorbers (iii), angle metal bracket (iv), vertically sliding metal plate (v).

i) A hemispheric silicone layer (radius 10 mm, thickness 6 mm) with squared base (side 24 mm, thickness 4 mm) simulates the viscoelastic properties of the finger. The choice of silicone type, mass and shape has great impact on the exposed characteristics of the device such as its stiffness, damping and inertia. The current prototype mounts soft silicone (Silastic 3481) having mass 4 g, young modulus 0.93 MPa and shore-A hardness 25. In III-B a comparison is reported with a harder silicone (Sylgard 184) having young modulus 1.45 MPa and shore-A hardness 40.

ii) A CZL635 load-cell monitors the exerted pressing force. The analog force signal is processed by a INA125P amplifier and sampled with 10-bit resolution by the Arduino ADC converter. The amplifier gain was set to read force values in the 0-20 N range with 0.1 N resolution. Although the load-cell can read values up to 50 N, greater values were considered outside the scope of our application.

iii) A pair of rubber shock-absorbers connect the end-effector to the linear motion actuator, preventing external vibration noise from reaching the accelerometer during measurements.

Three buttons, labeled *Up*, *Down*, *Stop/Function*, offer basic on-board controls, while a switch enables/disables the motor (e.g., once a target force is reached) making the device

completely silent and vibration-free. A 16×2 LCD display connected to the I2c bus of the Arduino provides various information to the user.

Mechanical supports and electronics lay on a thick wooden board. In our test setup, the device was fixed to a vibration-isolation table (CleanBench TMC).

B. Force Calibration

The load-cell was calibrated by measuring the forces exerted by the end-effector on a Kern 440-47 N digital scale: the output voltage of the load-cell was associated to the weight measured by the digital scale. The interpolation of multiple measurements resulted in two different model fits: due to the nonlinear behavior of the load-cell for values between 0 and 3 N, a 3rd-order polynomial was fitted in this range, whereas a linear model was adopted for higher forces.

Once a target force is reached by pressing against a surface, negative drifting may take place over time due to mechanical backlashes, proportionally to the magnitude of the applied force. To counteract such effect, the force-control algorithm overshoots the desired force by about 5% and then adjusts the end-effector's displacement until a stable force is reached.

C. Controls

The Arduino board processes both on-board and remote commands. A reduced set of commonly used functions is available on-board, operated by the device's physical buttons: i) read the current force at the end-effector; ii) set a target force level to be reached and held; iii) freely move the end-effector; iv) set the home/zero position.

Remote control is provided through the Arduino USB serial connection. The on-board functions are also made directly available through remote commands. Communication with the device is asynchronous, while the data type depends on the selected function mode. Three types of messages can be exchanged: force values, command acknowledgments and events. A remote control API is offered, implemented using Python 3.6 and OSC..[2] Example applications are supplied which showcase the device's functionalities.

III. Validation

The behavior of the *Bogus Finger* was analyzed and compared to that of the human finger.

A. Static Conditions

Considering contact against a stationary rigid surface, the stiffness exhibited by the end-effector – calculated as the ratio between the applied pressing force and the resulting displacement measured by counting the number of motor steps along the slide stroke – depends on the material and shape of its components.

[2] A widely used communication protocol optimized for multimedia and networking technology: http://opensoundcontrol.org/

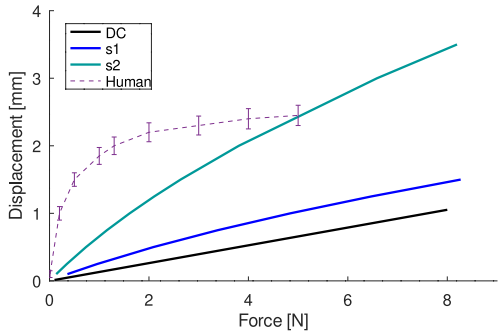

Fig. 2. Displacement of the end-effector as function of the normal force applied to a stationary rigid surface. The plots respectively show the effects of direct contact of the load cell (DC), and use of two different silicone layers at the interface (s1: Sylgard 184; s2: Silastic 3481). The force/deformation curve of the human fingertip as measured in [14], [16] is shown in dashed line.

Without a silicone interface, as in Fig. 1(a), the only compliant component is represented by the two shock-absorbers (i.e., the joint between the motor and the end-effector) which show a linear dependency between force and displacement (DC curve in Fig. 2).

Conversely, the addition of a hemispherical silicone layer at the interface introduces a nonlinear behavior (s1 and s2 curves in Fig. 2) caused by the increment of the contact area with the applied pressing force. The lower stiffness coefficient when using silicone layers strongly depends on their characteristics: they roughly behave as a spring in series with the shock-absorbers, and they are much more flexible than the latter.

B. Dynamic Conditions

Considering pressing against a rigid vibrating object, the impedance of the *Bogus Finger* at the contact point is determined by its inertia, stiffness and damping. Moreover, different pressing forces modify the stiffness and damping coefficients, thus affecting the frequency response of the vibrating object [11]: by analyzing such response for varying pressing forces it is therefore possible to evaluate the nonlinear stiffness and damping of the *Bogus Finger*, mainly introduced by its silicone interface.

For this purpose a testbed was designed based on a suspended and isolated 3D-printed PLA cuboid (side length 26 mm) housing two perpendicular actuators (Lofelt L5, peak resonance at 64 Hz), respectively vibrating vertically and horizontally (see Fig. 3).

Concerning the choice of force levels, preliminary tests with human participants showed high variability and fatigue for values greater than 5 N, therefore the following levels were selected: 0.5, 1, 2 and 4.9 N. As test vibrations, 250 Hz sinusoidal signals lasting 3 s (at 6 amplitude levels) and logarithmic sine sweeps between 10 and 600 Hz lasting 15 s (two repetitions) were used. While the latter account for the overall response of the system [23], the former allowed to assess more precisely the effect of pressing forces at the frequency of peak human sensitivity to vibration [9]. Vibrations were recorded with a PCB 356A17 triaxial accelerometer fixed to the top of the cuboid (see Fig. 3).

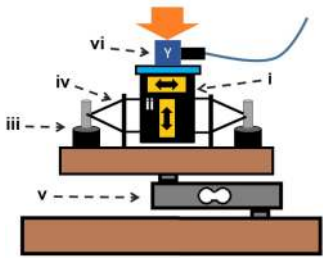

Fig. 3. Testbed used for validation: a PLA cuboid (i) housing two perpendicular actuators (ii) is suspended on rubber shock-absorbers (iii) through nylon wires (iv) by means of through-holes. The structure lays on a load-cell (v) measuring the applied normal force. Pressing forces are applied directly on top of an accelerometer (vi) fixed to the contact plate. .

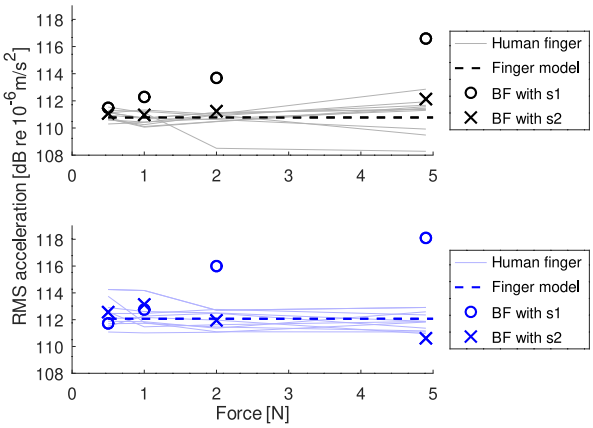

Fig. 4. Comparison of the different agents pressing on the testbed reproducing 250 Hz sinusoidal vibration through the vertical (above) or the horizontal (below) actuator. Human finger data are shown by thin solid lines, while the fitted linear models are plotted in dashed lines.

Ten participants (9 male, 1 female) were asked to reach and hold an assigned target force by pressing the index finger of their dominant hand on top of the accelerometer while vibration was provided. Visual feedback displayed on a computer screen guided them toward the target. The same procedure was repeated using the *Bogus Finger* with silicone layers s1 and s2. Pressing forces were recorded during the whole validation for assessing accuracy and precision.

The collected vibration (acceleration) recordings were analyzed to determine the effect of the following factors: agent (human subject, *Bogus Finger*), pressing force (range 0.5-4.9 N) and stimuli direction (vertical, horizontal). Results are reported below for the two vibration signals used in the test.

1) Response to 250 Hz Sinusoidal Vibration: For each stimulus, vibration acceleration data were analysed by calculating the median RMS of eight subsequent time windows lasting 0.2 s, so as to cancel out possible noise due to small unwanted movements of the participants during the acquisition. Fig. 4 reports the RMS acceleration for each agent relatively to the vertical and horizontal actuators. For each participant a linear model could be fitted, showing that, in the considered force range, vibration amplitude is not affected by the varying pressing forces. Similarly, the *Bogus Finger* with silicone s2 exposes a fixed mass that results in quasi-constant acceleration.

2) Response to Sine Sweep Vibration: For each measurement, the transfer function from the input signal to the output acceleration was calculated using the function `tfestimate` of the GNU Octave 5.1 software.

Fig. 5 compares the frequency responses of the human finger (dashed lines) to that of the *Bogus Finger* with silicone s1 and s2 for all factor combinations (4 force levels $\times$ 2 directions). The data measured from human subjects were aggregated in magnitude averages and standard deviations, providing more simple visualization and comparison.

The responses to human fingers (gray and blue areas) show a generally narrow confidence interval, especially in the range 200–400 Hz; in the same range, the response to the *Bogus Finger* with silicone s2 is rather close to that of the finger, with magnitude differences within ± 3 dB from the average. Conversely, in the lower range the response to our device diverges noticeably, and differences are greater with silicone s1 than s2 for all factor combinations. The most prominent difference involves the amplitude and frequency of the main resonance peaks, which are generally higher for the *Bogus Finger*. The amplitude of the main resonance peak depends mainly on the damping at the contact point, with low damping coefficients associated to large amplitudes; similarly, the frequency of the peak is proportional to the interface stiffness. Indeed, the harder silicone s1 always shows higher frequency peaks as compared to the softer silicone s2. Finally, vibration direction also affects the frequency response: for vertical vibration, the main peaks related to the *Bogus Finger* (for both silicone s1 and s2) occur at higher frequency than those associated with the human finger; instead, for horizontal vibration, the peaks related to the *Bogus Finger* and silicone s2 are close in frequency to those associated with the human finger, whereas their amplitudes are about 6 dB higher.

3) Pressing Force Control: Force-control error was analyzed in the data recorded during the experiment. Table I reports means and standard deviations of the normalized control error for human participants and the *Bogus Finger*. Means account for the accuracy of the pressing force, whereas standard deviations are related to the force-control precision. Overall, the best accuracy and precision are associated with the 2 N force level. For lower forces, the accuracy of human participants and the *Bogus Finger* are similar, while the precision of the device is much higher. When applying the highest pressing force (4.9 N) humans show the lowest accuracy, while the device shows uniformly high accuracy and precision for forces ≥ 2 N.

IV. Discussion

As Figs. 4 and 5 show, the validation of our tool reveals a good approximation of the human finger impedance in the frequency range 200–400 Hz. Below 200 Hz, however, our device exhibits a dissimilar mechanical impedance: its responses show additional resonance peaks not present with human fingers or having different frequency/amplitude. Each peak in the frequency response can be ascribed to a separate

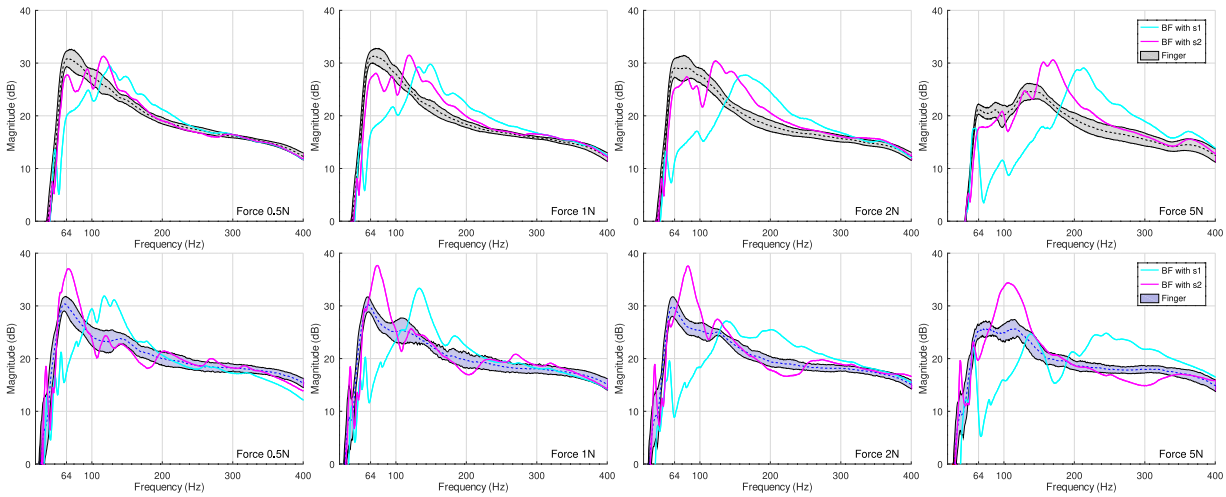

Fig. 5. Comparison of frequency responses of the testbed in the vertical (above) and horizontal (below) direction, for different pressing forces. The responses related to human participants are represented by grey (above) or blue (below) shaded areas, while the respective average responses are depicted by dashed lines. Solid cyan and magenta lines respectively report the response to the *Bogus Finger* with silicone s1 and s2.

TABLE I
FORCE-CONTROL ERROR

Force (N)	Error (%) mean ± s.d.	
	Human finger	*Bogus Finger*
0.5	1.6 ± 7.0	1.0 ± 1.6
1.0	-1.6 ± 4.7	1.0 ± 1.0
2.0	-1.1 ± 4.4	0.2 ± 0.25
4.9	-2.7 ± 3	-0.6 ± 0.6

inertial component connected to the system through a spring-damper joint; The peak frequency mainly depends on the ratio between stiffness and mass, whereas its magnitude is inversely proportional to the damping coefficient [11]. Such factors are separately analyzed in what follows.

A. *Stiffness and Mass*

As highlighted in Fig. 2, the stiffness exposed by the *Bogus Finger* mainly depends on the properties of its silicone interface; thus, its hardness and shape could be adapted so as to match a desired stiffness characteristic.

The stiffness of the finger in the normal direction is usually measured by compressing the fingertip while holding it still; the resulting deformation grows quickly, then shows an asymptotic trend [14], [16]. By contrast, the displacement of the *Bogus Finger* is measured along its linear slide, hence accounting for deformation both at the silicone interface (fingertip emulation) and at the shock-absorbers (representing the metacarpophalangeal joint). Measurements made by extending the whole finger [6] show a trend similar to that of the *Bogus Finger*, yet with a greater displacement magnitude due to the softness of phalanx's joints, whereas our device does not emulate them but rather represent the finger as a whole.

The finger-analogue implementations described in the literature (e.g., [20], [21]) mainly address the quasi-static properties of the human finger, thus simulating the local properties of the fingertip pulp rather than the entire finger. As a result, a direct comparison between those finger-analogues and our device is unpractical, especially with regard to the modeled stiffness. Anyhow, similar to the *Bogus Finger*, those finger-analogues also show greater stiffness as compared to the human finger.

The mass exposed by the finger depends on the stimuli direction: its inertia is about 6 g in the normal direction [6] and less than 0.5 g in the lateral one [7]. By contrast, the *Bogus Finger* comprises multiple inertial components, which are especially emphasized by vibratory inputs below 200 Hz: in that range vibrations propagate to the entire structure, setting those components into oscillation and causing unwanted resonances. On the other hand, thanks to the low stiffness of the silicone layer and the greater mass of the end-effector, the only inertial component affected by vibrations above 200 Hz is the mass of the silicone layer; similar to the human finger, there the *Bogus Finger* exhibits a small constant inertia regardless of the applied force.

The shift of resonance peaks towards higher frequencies, visible in Fig. 5, is proportional to the increase of the contact area and the stiffness growth consequence of the applied force. With regard to vertical vibration, the frequency of the peaks confirms the larger stiffness of the *Bogus Finger* as compared to human fingers, especially when low-magnitude forces are applied. Concerning horizontal vibration, instead, our device results in resonances with frequencies that are more similar to those caused by human fingers. Unlike the *Bogus Finger*, human fingers show negligible stiffness increments up to 2 N: this may be ascribed to the low friction of the accelerometer's surface, resulting in slip effects when limited fingertip compression occurs.

B. *Damping*

The damping coefficient of the human finger varies between 1-4 N · s/m and increases proportionally with the applied force for both normal and lateral vibration directions [6], [7]. Based

only on the responses reported in Fig. 5, a precise measurement of the damping exposed by the *Bogus Finger* cannot be obtained. However, by comparison with the recorded responses of human fingers, we can speculate that the prominent peaks within 60–200 Hz are most likely related to a lower damping coefficient of the silicone interface, especially in the horizontal direction.

V. Conclusion

We presented design aspects and key features of the *Bogus Finger*, a robotic tool which simulates a human finger applying quasi-static forces on stationary or vibrating surfaces. Future extensions encompass the simulation of force envelopes by means of lookup tables directly controlling the motion of the stepper motor: these would allow to achieve increased acceleration/velocity (e.g., reproducing impacts) at the expense of spatial accuracy, which could however be recovered via force-feedback control.

The validation of our prototype revealed good approximation of the finger impedance in the frequency range of highest human sensitivity to vibration. Despite this, its impedance diverges in the lower range, with resonance peaks either located at higher frequency or having larger amplitude respectively for vertical or horizontal vibration. Those peaks may be made to match the response of the human finger by fine-tuning the silicone layer in its mass, stiffness, damping and form factor parameters, possibly making use of composite materials [22]. To achieve this goal, however, the contribution of each element of the end-effector needs to be precisely assessed and modeled. To this end, numerical simulations could be used to fine-tune its parameters while reducing the number of tests with physical prototypes [21]. In this perspective, a detailed mechanical model of the current prototype is currently being developed and parametrized.

The availability of our low-cost DIY tool in open-access form, rather than proprietary and expensive finger-analogues, has the potential to grant access to realistic simulation of finger-based interactions to a larger community of researchers in the fields of touch psychophysics and haptic interfaces.

References

[1] S. Papetti, H. Järveläinen, B. L. Giordano, S. Schiesser, and M. Fröhlich, "Vibrotactile sensitivity in active touch: Effect of pressing force," *IEEE Trans. Haptics*, vol. 10, no. 1, pp. 113–122, Jan.–Mar. 2017.

[2] G. H. Van Doorn, V. Dubaj, D. B. Wuillemin, B. L. Richardson, and M. A. Symmons, "Cognitive load can explain differences in active and passive touch," in *Haptics Perception, Devices, Mobility, Commun., Ser. Lecture Notes in Computer Science*, P. Isokoski and J. Springare, Eds. Berlin, Heidelberg: Springer Berlin Heidelberg, 2012, vol. 7282, pp. 91–102.

[3] T. E. Milner and D. W. Franklin, "Characterization of multijoint finger stiffness: Dependence on finger posture and force direction," *IEEE Trans. Biomed. Eng.*, vol. 45, no. 11, pp. 1363–1375, Nov. 1998.

[4] S. Oh and S. Choi, "Effects of contact force and vibration frequency on vibrotactile sensitivity during active touch," *IEEE Trans. Haptics*, vol. 12, no. 4, pp. 645–651, Oct.–Dec. 2019.

[5] C. Hatzfeld and R. Werthschützky, "Mechanical impedance as coupling parameter of force and deflection perception: Experimental evaluation," in *Proc. Int. Conf. Hum. Haptic Sens. Touch Enabled Comput. Appl.* 2012, pp. 193–204.

[6] A. Z. Hajian and R. D. Howe, "Identification of the mechanical impedance at the human finger tip," *J. Biomechanical Eng.*, vol. 119, no. 1, pp. 109–114, Feb. 1997.

[7] M. Wiertlewski and V. Hayward, "Mechanical behavior of the fingertip in the range of frequencies and displacements relevant to touch," *J. Biomech.*, vol. 45, no. 11, pp. 1869–1874, 2012.

[8] E. Concettoni and M. J. Griffin, "The apparent mass and mechanical impedance of the hand and the transmission of vibration to the fingers, hand, and arm," *J. Sound Vib.*, vol. 325, no. 3, pp. 664–678, 2009.

[9] R. T. Verrillo, "Vibration sensation in humans," *Music Percep.: An Interdiscipl. J.*, vol. 9, no. 3, pp. 281–302, 1992.

[10] S. Papetti, H. Järveläinen, and S. Schiesser, "Interactive vibrotactile feedback enhances the perceived quality of a surface for musical expression and the playing experience," *IEEE Trans. Haptics*, to be published, doi: 10.1109/TOH.2021.3060625.

[11] T. A. Kern and R. Werthschützky, "Studies of the mechanical impedance of the index finger in multiple dimensions," in *Proc. Int. Conf. Hum. Haptic Sens. Touch Enabled Comput. Appl*. 2008, pp. 175–180.

[12] T. T. Diller, "Frequency response of human skin in vivo to mechanical stimulation," Master's thesis, Massachusetts Inst. Technol., USA, 2001.

[13] D. T. Pawluk and R. D. Howe, "Dynamic contact of the human fingerpad against a flat surface," *J. Biomechanical Eng.*, vol. 121, no. 6, pp. 605–611, 1999.

[14] E. R. Serina, E. Mockensturm, C. D. Mote, and D. Rempel, "A structural model of the forced compression of the fingertip pulp," *J. Biomech.*, vol. 31, no. 7, pp. 639–646, 1998.

[15] J. Z. Wu, D. E. Welcome, K. Krajnak, and R. G. Dong, "Finite element analysis of the penetrations of shear and normal vibrations into the soft tissues in a fingertip," *Med. Eng. Phys.*, vol. 29, no. 6, pp. 718–727, 2007.

[16] H.-Y. Han and S. Kawamura, "Analysis of stiffness of human fingertip and comparison with artificial fingers," in *Proc. IEEE SMC'99 Conf. Proc. 1999 IEEE Int. Conf. Syst., Man, Cybern. (Cat. No 99CH37028)*, 1999, vol. 2, pp. 800–805.

[17] M. C. Haverkamp, "Effects of material touch sounds on perceived quality of surfaces," *SAE Int. J. Mater. Manuf.*, vol. 10, no. 2, pp. 182–190, 2017.

[18] N. Wettels, V. J. Santos, R. S. Johansson, and G. E. Loeb, "Biomimetic tactile sensor array," *Adv. Robot.*, vol. 22, no. 8, pp. 829–849, 2008.

[19] R. S. Dahiya, G. Metta, M. Valle, and G. Sandini, "Tactile sensing-from humans to humanoids," *IEEE Trans. Robot.*, vol. 26, no. 1, pp. 1–20, Feb. 2010.

[20] R. Fenton Friesen, M. Wiertlewski, M. A. Peshkin, and J. E. Colgate, "Bioinspired artificial fingertips that exhibit friction reduction when subjected to transverse ultrasonic vibrations," in *Proc. IEEE World Haptics Conf.*, 2015, pp. 208–213.

[21] M. Controzzi, M. D'Alonzo, C. Peccia, C. M. Oddo, M. C. Carrozza, and C. Cipriani, "Bioinspired fingertip for anthropomorphic robotic hands," *Appl. Bionics Biomech.*, vol. 11, no. 1, 2, pp. 25–38, 2014.

[22] A. K. Dabrowska *et al.*, "Materials used to simulate physical properties of human skin," *Skin Res. Technol.*, vol. 22, no. 1, pp. 3–14, 2016.

[23] A. Farina, "Advancements in impulse response measurements by sine sweeps," in *Audio Eng. Soc. Conv. 122*, paper 7121 Audio Eng. Soc., 2007.